Intracellular expression of arginine deimimase activates the mitochondrial apoptosis pathway through inhibiting cytosolic ferritin and inducing chromotin autophagy

Qingyuan Feng
Department of Otorhinolaryngology Head and Neck Surgery, the First Affiliated Hospital of Guangxi Medical University
Xuzhao Bian
State Key Laboratory of Virology, College of Life Sciences, Wuhan University
Xuan Liu
State Key Laboratory of Virology, College of Life Sciences, Wuhan University
Ying Wang
State Key Laboratory of Virology, College of Life Sciences
Huiting Zhou
State Key Laboratory of Virology, College of Life Sciences
Xiaojing Ma
State Key Laboratory of Virology, College of Life Sciences
Chunju Quan
State Key Laboratory of Virology, College of Life Sciences
Yi Yao
Department of Oncology, Renmin Hospital of Wuhan University
Zhongliang Zheng (biochem@whu.edu.cn)
College of Life Sciences in Wuhan University https://orcid.org/0000-0003-2861-5720

Research article

Keywords: Arginine deprivation, arginine deiminase, apoptosis, mitochondria damage, chromotin autophagy

Posted Date: April 17th, 2020

DOI: https://doi.org/10.21203/rs.2.22978/v2

Version of Record: A version of this preprint was published on July 16th, 2020. See the published version at https://doi.org/10.1186/s12885-020-07133-4.

Abstract

Background Based on its low toxicity, arginine starvation therapy has the potential to treat those malignant tumors that can't be treated by surgery. Arginine deiminase (ADI; EC 3.5.3.6) gene is indicated to be an ideal cancer-suppressor gene. ADI expressed in cytosol displayed higher oncolytic efficiency than ADI-PEG20 (Pegylated Arginine Deiminase by PEG 20,000)[1]. However, it is still unknown whether cytosolic ADI has the same function mechanism as ADI-PEG20 or other underlying mechanisms in cells.

Methods The interaction of ADI and other protein factors was screened by yeast hybrid, and verified by co-immunoprecipitation and immunofluorescent staining. The effect of ADI inhibiting ferritin light-chain domain (FTL) on mitochondria damage was evaluated by site-directed mutation and flow cytometry. The apoptosis pathway of mitochondria control was analyzed by Western Blot and real-time PCR. The effect of p53 expression on cancer cell death was assessed by siTP53 transfection. The chromatin autophagy was explored by immunofluorescent staining and Western Blot.

Results ADI expressed in cytosol inhibited the activity of cytosolic ferritin through interacting with FTL. The inactive mutant of ADI still aroused the apoptosis of some cells through mitochondria damage. Arginine deprivation also induced the expression increase of p53 and p53AIP1, which aggravated cellular mitochondria damage. Chromatin autophagy appeared at the later stage of arginine deprivation. DNA damage came along with the whole process of arginine starvation. Histone 3 (H3) was found in autophagosomes, which implied that cancer cells try to utilize the arginine in histones to survive during arginine starvation.

Conclusions Mitochondria damage is the major mechanism for ADI expressed in cytosol to induce cancer cell death. Chromatophagy accumulation not only drives cancer cell to utilize histone arginine but also speeds up cancer cell death at the later time point of arginine deprivation.

Background

Tumor starvation therapy has become a mainstream target strategy for cancer therapy in clinic. In addition to the starvation therapy of angiogenesis inhibition[2], the deprivation of specific amino acid is also a potential cancer therapy. ADI gene is from *Mycoplasma*. ADI catalyzes the conversion of arginine to citrulline. As a potential anti-cancer drug, ADI-PEG20 already obtained some good results in Phase I and II clinic studies[3, 4]. When injected intravenously, ADI-PEG20 depletes the arginine in blood to starve some specific tumors. Those tumors can't synthesis arginine due to the deficiency of argininosuccinate synthetase (ASS)[5]. David K. Ann and Hsing-Jien Kung[6, 7] et al. described how ADI-PEG20 produced arginine deprivation *in vitro* to specifically kill tumor cells by a novel mechanism involving mitochondria dysfunction, reactive oxygen species generation, nuclear DNA leakage and chromatin autophagy. DNA damage caused by chromatin autophagy triggered the death of cancer cells. However, ADI-PEG20 displayed lower efficiency of oncolysis. Arginine deprivation in blood only continued for two weeks in an ASS1-methylated malignant pleural mesothelioma[8]. Then, plasma arginine levels recovered due to the

development of anti-ADI neutralizing antibodies at the fourth week[8]. ADI-PEG20 monotherapy did not demonstrate an overall survival benefit for hepatocellular carcinoma (HCC) in Phase III clinic studies [9]. Therefore, new strategies are needed to synergize the effect of ADI-PEG20 in or transform the using way of ADI gene.

ADI gene is a potential cancer suppressor gene[1]. ADI expressed in cytosol displayed higher apoptosis-inducing efficiency than ADI-PEG20. Cytosolic ADI quickly exhausted the arginine in cytoplasm[1], and then caused fast cancer cell death. ADI adenovirus also presented excellent oncolytic efficiency[1]. Moreover, the promoter of human telomerase reverse transcriptase (hTERT) was utilized to control ADI expression in adenovirus, which ensured higher safety for normal cells.[1] However, it is still unknown whether cytosolic ADI has certain potential interactions in cells, or how the cells respond to rapid endogenous arginine deprivation. The solution of these problems will effectively prevent side effects when ADI gene is used for cancer gene therapy in future.

FTL was screened out by yeast two-hybrid. cytosolic ADI was proved to interact with FTL in cytoplasm. Cytosolic ferritin functions as storage and transport of iron ions in cells. In order to eliminate the lethal effect of ADI enzyme activity on cancer cells, we mutated the catalytic residue of ADI into alanine. Thus, the interaction of ADI and FTL was found to have only very limited lethal effect on tumor cells. Then, we detected the apoptosis pathway of mitochondria control. The increasing expression of p53 and p53AIP1 led to mitochondria damage at the early stage of arginine deprivation. At the later time of arginine deprivation, chromatin autophagy became worse and aggravated the mitochondria damage.

The molecular mechanism of cell death induced by ADI expressed in cytosol was proved here to be associated with some cellular dysfunctions including ferritin inhibition, p53 expression upregulation, DNA damage and chromatin autophagy. The interaction of ADI and FTL had not been shown to be the dominant reason of mitochondria damage. Arginine deprivation was still the key mechanism for ADI to suppress tumors. In addition, cytosolic ADI was found not to interact with other cellular factors, which suggested its potential drug safety.

Methods

Plasmid construction

To construct pcDNA4-ADI, an ADI-overexpressing plasmid, ADI coding sequence was synthesized by Nanjing Genscript LTD and sub-cloned into the *EcoR* I/*Xho* I sites of pcDNA^{TM}4/TO/myc-His vector. C-myc tag was fused at the c-terminal of ADI protein. Two primers were used (5'-GATATGAATTCACCATGTCCGTCTTCGAT AGCAAGT -3' and 5'- GATATCTCGAG TCACCATTT GACATCTTTTCTGGACA -3'). pcDNA4-ADI△(cysteine398alanine) plasmid was constructed through overlapping extension method. Two mutant primers were used (5' GTATGGGTAACG CTCGTGCCATGTCAATGCCTTTATC 3' and 5' GATAAAGGCATTGACATGG CACGAGCGTTACCCATAC 3').

To build pGBKT7-ADI plasmid as screening bait in yeast hybrid experiment, ADI coding sequence was inserted into the Nde I/BamH I sites of pGBKT7 vector which expresses proteins fused to amino acid 1-147 of the GAL4 DNA binding domain. Two primers were used (5'-GATATCATATGTCCGTCTTCGATAGCAAG TT -3' and 5'- GATATCTCGAGTCACCATTT GACATCTTTTCTGGACA -3').

Other plasmids were donated by Dr. Youjun Li in Life Science College of Wuhan University.

Cell culture and transfection

Human liver cancer cell lines (HpG2), Prostate cancer cell line (PC3) and human embryo lung cell line (MRC5) were cultured with DMEM supplemented with 10% fetal bovine serum (FBS), penicillin (100IU/ml) and streptomycin (100 μg/ml). Cells were grown in a 5% CO2 cell culture incubator at 37℃. All culture reagents were purchased from Life Technologies LTD.

Lipofectamine™ 2000 Transfection Reagent (Cat. #11668019) was from ThemoFisher Scientific. Transfection was performed according to the manufacturer's instructions. For siRNA transfection, siRNA specific for TP53 (5'- ACCUCGGAAGACUCCAGUGGUAAUCUUCAAGAGAGAUUACCACUGGAGUCUUCCUU-3' / 5'- CAAAAAGGAAGACUCCAGUGGUAAUCUCUCUUGAAGAUUACCACUGGAGUCUUCCG-3'), or TP53AIP1 (5'- ACCUCGGGAAUAGAAGCUCUGUCAGUUCAAGAGACUGACAGAGCUUCUAUUCCCUU-3' / 5'-CAAAAAGGGAAUAGAAGCUCUGUCAGUCUCUUGAACUGACAGAGCUUCUAUUCCCG-3'), or non-specific control (5'-UAAUGUAUUGGAACGCAUAUU-3'/5'-UAUGCGUUCCAAUACAUUA-3') was co-transfected into HepG2 or PC3 cells by using the Lipofectamine 2000. Immunoblots and FACS analyses were performed 2 days after transfection

Yeast Two-Hybrid Assay

Yeast two-hybrid analysis was performed in *yeast strain AH109* according to the manufacturer's instructions (http://www.clontech.com/). pGBKT7-ADI plasmid as bait plasmid was co-transformed into AH109 yeast with the yeast two-hybrid cDNA library of human liver (Cat. #630468) from Clontech Laboratories Inc. Quadruple dropout medium (without tryptophan, leucine, histidine and adenine) containing 4mg/ml x-a-gal was used to test the activation of reported genes MEL1 (MDS1/EVI1-like gene 1).

Co-immunoprecipitation (co-IP)

pcDNA4-ADI plasmid had been transfected into HepG2 and PC3 cells for two days. Pierce Classic Magnetic IP/Co-IP Kit (Cat. #88804, ThermoFisher Scientific) was used for conjugating myc-tag antibody

(Cat. #16286-1-AP) or FTL antibody (Cat. # ab201975). The conjugated beads were placed into cell lysates containing ADI expression to capture the ADI-FTL complex. Then, beads were centrifuged, washed, and run SDS-PAGE gel for immunoblot staining.

Immunofluorescence Staining for co-localization.

HepG2 and PC3 cells were cultured on chamber slides for 24 h. Washed slides with PBS three times and transfected pcDNA4-ADI plasmid. Washed again after 2 days. The cells were then fixed with 4% paraformaldehyde for 1 hour at room temperature. After washing the slides twice with PBS, the cells were blocked with 10% FBS. The cells were then incubated with myc-tag antibody (Cat. #16286-1-AP) or FTL antibody (Cat. # ab201975) at room temperature for 1 hour. The slides were washed twice with PBS. TRITC conjugated goat anti-rabbit antibody (Cat. #A16101) and FITC conjugated goat anti-mouse antibody (Cat. #62-6511) were added and incubated at room temperature for 1 hour. The slides were then washed with PBS twice before the addition of DAPI. After additional washes with PBS, slides were mounted with Prolong Gold Antifade Reagent (Invitrogen). Immunofluorescence staining was examined under a confocal microscope.

RNA Isolation and Quantitative RT-PCR

Total RNA was extracted from cells using Trizol (Invitrogen) following the manufacturer's instructions. The RNA concentration and purity were determined by spectrophotometry (NanoDrop Technologies Inc., LLC). One microgram of total RNA was used as the template for synthesizing complementary DNA (cDNA) by using the cDNA Synthesis Kit (ThermoFisher Scientific). Quantitative RT-PCR (qRT-PCR) was performed by using SYBR Green PCR Master Mix with the StepOne Real-Time PCR System (Bio-Rad). $2^{-\triangle\triangle Ct}$ in relative quantification analysis method was used to calculate the change fold of mRNA among the different cells. GAPDH was utilized as an internal control for the normalization. The primers used for RT-PCR were listed in supplementary tab S1.

Western Blot Analysis

Five micrograms of protein were electrophoresed in 10% SDS-PAGE gels and blotted to polyvinylidine difluoride membranes. Specific primary antibodies were detected with peroxidase-labeled secondary antibodies (ProteinTech Group Inc.) by using SuperSignal West Dura Extended Duration Substrate (Pierce Chemical) per manufacturer's instructions. The used antibodies from ProteinTech Group Inc. included myc-tag antibody (Cat. #16286-1-AP), ASS antibody (Cat. #66036-1-Ig), GAPDH antibody (Cat. #60004-1-Ig), Flag-tag antibody (Cat. #66008-3-Ig), p53 antibody (Cat. #60283-2-Ig), Bcl-2 antibody (Cat. #60178-1-Ig), PUMA antibody (Cat. #55120-1-AP), Bax antibody (Cat. #60267-1-Ig), caspase 9 antibody (Cat.

#66169-1-Ig), caspase 3 antibody (Cat. #66470-2-Ig), Histone H3 antibody (Cat. #17168-1-AP), HRP-conjugated goat anti-mouse IgG (Cat. #SA00001-1) and HRP-conjugated goat anti-rabbit IgG (Cat. #SA00001-2). FTL antibody (Cat. #ab201975) was from Abcam Inc.. p53AIP1 antibody (Cat. #ABP56144) was from Abbkine Inc., Noxa antibody (Cat. #ab13654) was from Abcam Inc.. Bak antibody (Cat. #ab69404) was from Abcam Inc.. TRITC conjugated goat anti-rabbit antibody (Cat. #A16101) was from ThermoFisher Scientific Inc.. FITC conjugated goat anti-mouse antibody (Cat. #62-6511) was from ThermoFisher Scientific Inc..

Fluorescence assay for mitochondrial permeability transition pore (MPTP)

MPTP activation assay followed the manuscript of LIVE Mitochondrial Transition Pore Assay Kit (GMS10095.1 v.A) from GENMED SCIENTIFICS INC. U.S.A. Cells were inoculated in 96-well plates at a density of 5×10^4 cells per well, and transfected with pcDNA4-ADI plasmid. After incubation for 48h, cells were stained with 50μg calcein-AM (Calcein acetoxymethyl ester), washed with 0.1M phosphate buffer solution (PBS), and neutralize with 0.1M cobalt (II) chloride hexahydrate. Then detected fluorescence intensity of cells in Thermo Multiskan™ FC Microplate Reader.

GFP-LC3 reporter fluorescence assay for autophagy in live cells

Expression of the GFP-LC3 fusion gene allows to visualize autophagosome formation in real time in live cells. Firstly, cells were inoculated in twelve-well plates with cover slips at a density of 1×10^5 cells per well, and co-transfected with pcDNA4-ADI and pEGFP-LC3 plasmids. Secondly, cells were starved with serum-free medium for 72 hours. Thirdly, cells were fixed with 4% paraformaldehyde, permeabilized with 0.2% Triton X-100. Cellular nucleuses were stained by DAPI for 10 minutes. Finally, the plates were sealed and stored at 4℃. GFP fluorescent signals were detected by using a confocal microscope (LeicaMicrosystems, Mannheim, Germany).

Chromatin autophagy assay by fluorescence co-localization.

Cells were inoculated in twelve-well plates with cover slips at a density of 1×10^5 cells per well, and co-transfected with pcDNA4-ADI and pEGFP-LC3 plasmids. Then, 2% FBS was added into DMEM medium to prevent cells from dying too quickly. After 96 hours of culture time, cells were fixed with 4% paraformaldehyde, permeated with 0.2% Triton X-100. Then, cells were incubated with TRITC-labeled anti-H3 antibody for 4 hours at 4℃. After wash, cellular nucleuses were stained by DAPI for 10 minutes. Finally, the plates were sealed and stored at 4℃. Fluorescent signals were detected by using a confocal microscope

Statistical analysis.

Data with error bars are presented as mean ± S.D. Student's two-tailed t test was used to determine the p-value. Differences were considered statistically significant when the p-value was <0.05.

Results

Cancer cells apoptosis induced by ADI expressed in cytosol.

ADI expressed in cytosol will efficiently deplete intracellular arginine and lead to cell death. Thus, we transfected pcDNA4-ADI plasmid into cancer cells to express ADI and assessed apoptosis rate. Based on cancer tissue specificity of ASS expression[5], MRC5 cell line (ASS+) were used as the negative control, PC3 (ASS-) and HepG2 (ASS-) cell lines were used as research targets. As the immunoblotting dots shown in fig 1c and supplementary fig S1, ASS gene was silent in HepG2 and PC3 cells, but was highly expressed in MRC5 cells. As shown in figure 1a and 1b, ADI expression efficiently induced the death of PC3 and HepG2 cells two days after plasmid transfection. Mortality was calculated by summing the rates of early apoptosis cells, late apoptosis cells and dead cells. PC3 cell line displayed nearly 17% of cell death rate. HepG2 cell line also obtained almost 15% of death rate. However, MRC5 cell line showed about 4% of death rate. 200mg/L of arginine was used to counteract arginine deprivation aroused by cytosolic ADI. The DMEM medium containing 200mg/L of arginine was replaced every 24 hours after the transfection of pcDNA4-ADI plasmid. High concentration of arginine obviously reduced the death rates caused by cytosolic ADI. For example, HepG2 cells decreased its death rate to about 7.7% and PC3 cells decreased to about 8.0%.

The interaction of ADI and FTL promoted the mitochondria damage.

To understand whether cytosolic ADI has certain potential interactions, we screened protein factors possibly interacting with ADI by yeast hybrid method. A cDNA library of human liver from Clontech Laboratories Inc, was used as screening target. As shown in fig 2a, FTL was screened out and made yeasts display obvious green color on the selecting plate (SD/Gal/Raf/-Ura, -His, -Trp, -Leu) by interacting with ADI. Then, immunofluorescence staining was applied to detect intracellular co-localization of ADI and FTL. As shown in fig 2c, FTL located in cytoplasm which was labeled with FITC-green fluorescence. ADI positioned in the whole cell that was labeled with TRITC-red fluorescence. Obviously, the cytoplasm was their interaction place as shown from merged pictures. co-IP was done to further verify intracellular interaction of ADI and FTL. As shown in fig 2b and supplementary fig S2, FTL was check out by Western Blot experiment when ADI was used as IP bait. ADI was also detected by Western Blot experiment when FTL was IP bait.

The enzymatic activity of ADI was removed to accurately determine how cytosolic ADI caused cancer cell death by interacting with cytosolic FTL. The amino acid residue of cysteine398 is the catalytic residue of ADI[10]. We mutated cysteine398 into alanine398 to remove the enzymatic activity of ADI. pcDNA4-ADI△(C398A) plasmid was transfected into PC3 and HepG2 cells to detect cell apoptosis. pCMV-FTL plasmid was co-transfected to neutralize the action of cytosolic ADI△. As shown in fig 3a, 3b, 3d and supplementary fig S3, the cytosolic ADI△ still led to 13% of PC3 cell death, and 10% of HepG2 cell death after the transfection for 3 days. However, the over-expressed FTL obviously neutralized the death-induced effects on these two cells. The co-transfection of pcDNA4-ADI(C398△A398) and pCMV-FTL plasmids decreased the death rate of PC3 cells to about 7% and HepG2 cells to about 3%. MPTP experiments was further performed to verify the mitochondria damage caused by the cytosolic ADI△. As shown in fig 3c, the cytosolic ADI△ decreased half of fluorescence intensity of living cells stained by calcein-AM. The co-transfected cells almost kept the same fluorescence intensity as the control cells. Thus, FTL overexpression in cells prevented the mitochondria damage aroused by the cytosolic ADI.

Mitochondria apoptosis pathway induced by arginine deprivation in cells

Apoptosis pathways of mitochondria control were explored by fluorescent quantitation RT-PCR and Western Blot experiment. As shown in fig 4a, the mRNA levels of some important factors increased after ADI was expressed in cells for 2 days, such as FTL (about 1.5 fold), p53 (about 1.5 fold), p53AIP1 (about 4.5 fold), Noxa (about 6.0 fold), PUMA (about 1.5 fold), CASP9 (about 3.0 fold) and CASP3 (about 7.0 fold). As show in fig 4b, 4e, 4f and supplementary fig S4, the protein levels of these factors also increased after 2 days of arginine deprivation. However, Bax and Bak increased their protein levels at the fourth day of ADI expression. As shown in fig 4c, mitochondria damage was verified by MPTP experiments. Fluorescence intensity of living cells stained by calcein-AM decreased hardly after 2 days or 4 days of arginine deprivation. As shown in fig 4d and 4e, the activities of CASP3 and CASP9 were also increased for about 1.5 to 2.0 fold at same time.

The increased p53AIP1 will activate the p53-dependent apoptosis[11]. Thus, we respectively knocked down p53 mRNA and p53AIP1 mRNA to verify their function in mitochondria damage during arginine deprivation. As shown in fig 5d and 5e, the protein levels of p53 and p53AIP1 decreased in PC3 and HepG2 cells after 2 days of arginine deprivation and siRNA transfection. The knock-down of p53 mRNA level effectively decreased cell death rates, as flow cytometry results displayed in fig 5a and 5b, siTP53AIP1 also reduced cell death rates in PC3 and HepG2 cells. MPTP experiments displayed the same results as shown in fig 5c. Fluorescence intensity of living cells stained by calcein-AM were much higher in siRNA-treated cells than in scrRNA-treated cells.

Cellular autophagy induced by ADI expressed in cytosol.

Cellular autophagy was detected because nutrient starvation is the major reason to trigger excessive autophagy[12]. Assay for microtubule-associated protein 1A/1B-light chain 3 (LC3) is the basic protocol for the detection of autophagosome. A cytosolic form of LC3 (LC3-I) is conjugated to phosphatidylethanolamine to form LC3-phosphatidylethanolamine conjugate (LC3-II) during autophagy, which is recruited to autophagosomal membranes. Thus, assay for the formation of GFP-LC3-II can reflect starvation-induced autophagic activity.[13].

pcDNA4-ADI plasmid and pEGFP-LC3 plasmid were co-transfected into MRC5, PC3 and HepG2 cell lines. After 96h, GFP fluorescence was detected by a confocal microscope. The protein levels of LC3 were verified by Western Blot experiment at the same time. As shown in fig 6b, 6c and supplementary fig S6A, LC3-II proteins were detected only in HepG2 and PC3 cells expressing ADI proteins. The autophagosomes also appeared in these cells expressing ADI proteins as shown in fig 6a. However, MRC5 cells did not show any autophagosomes during arginine deprivation. At the same time, the protein expression of histone 3 (H3) was checked out by Western Blot experiment. H3 protein level decreased hardly after 96 hours of arginine deprivation as shown in fig 6d, 6e and supplementary fig S6B.

Chromatin autophagy was further detected through fluorescence co-localization technology. As shown in fig 6f, cell nucleus presented budding phenomenon in HepG2 and PC3 cells. There were some autophagosomes appearing in the cytoplasm. The merged pictures displayed that DNA fragments, GFP-LC3-II and histone H3 located in the same autophagosomes.

Discussion

Tumors are very smart, which will actively adapt to the changes of microenvironments when they are threatened by death. In clinic, some tumors always stay in quiescent condition because of the hypoplasia of their blood vessels. Some tumor tissues remain in hunger since they can not obtain enough nutrient substances through hypoplastic blood vessels. What's more, selectively starving cancer cells can also make tumors keep in hunger, which is the metabolic-based therapy for cancers with tiny side effects. Cancer-starving therapies, such as dietary modification, tumor angiogenesis inhibition and aspartic acid deficiency, can effectively decrease the incidence of spontaneous tumors and slow the growth of primary tumors[14].

ADI was a good gene with the potential for cancer gene therapy. As the description of our preliminary work[1], ADI expressed in cytosol was proved to possess higher apoptosis-inducing efficiency, tumor-targeting specificity, and oncolytic activity[1]. In order to exclude the actions of adenovirus on cells, we just used pcDNATM4/TO/myc-His vector as ADI expression vector without replacing pCMV promoter with phTERT promoter. Rapid growth of tumors requires a lot of nutrition including arginine. Tumor cells with ASS gene deficiency are more sensitive to arginine deprivation than normal cells, for example endometrial cancer[15]. Based on cancer tissue specificity of ASS expression[5], we used MRC5 (ASS+), PC3 (ASS-) and HepG2 (ASS-) cell lines to explore whether ADI had the same effect on different cancer cell lines. As shown in fig 1, ADI expressed in cytosol eventually induced cellular apoptosis of PC3 and HepG2 cells.

ADI-PEG20 had been proved to induce cellular autophagy and caspase-independent apoptosis through exhausting the arginine in blood[16]. However, it is unknown whether cytosolic ADI has the same or unique anti-tumor mechanism in cells. Therefore, FTL as an interacting target was screened out by yeast hybrid method as shown in fig 2. Co-IP results proved the interaction of ADI and FTL in cells. Fluorescence co-localization showed that the interaction happened in the cytoplasm.

Ferritin is considered the major iron storage protein, which participates the regulation of cellular iron homeostasis[17]. Mitochondrial function also requires iron replenishment from cytoplasmic ferritin. The inhibition of ferritin directly results in the dysfunction of mitochondrial electron transport[18]. In order to exclude the effect of ADI enzyme activity on cell function, the catalytic residues of ADI were mutated to alanine residues. Cysteine398, the catalytic residue of ADI[10], was mutated into alanine398. Since alamine398 as an inert residue has no nucleophilic catalytic capacity, the mutation (C398△A398) effectively terminated the enzyme activity of ADI[19]. As shown in fig 3, ADI△(C398△A398) still caused a small number of cell death in PC3 and HepG2 cells. The overexpression of FTL neutralized the death-induced effects on these two cells. We speculated that FTL overexpression made up the part of cytosolic FTL that has lost its function due to interaction with ADI. However, after plasmid transfection, ADI△(C398△A398) required expression for 3 days to induce cancer cell death, but ADI only needs 2 days as shown in fig 1. Obviously, cytosolic ADI△ just induces limited apoptosis through interacting with cytosolic FTL. Thus, the interaction of ADI and FTL is not the main reason of mitochondria damage. In addition, as shown in Fig. 1, the high concentration of arginine in the culture medium counteracted the cell death caused by ADI expressed in cytosol. This result further demonstrates that arginine deprivation in cells is the main mechanism for cytosolic ADI to suppress cancer cells.

Accumulating evidences in research papers have illustrated that arginine deprivation *in vitro* exerts its anticancer effects in various tumors by inducing mitochondrial damage and autophagy[6, 7, 20, 21]. Arginine deprivation inhibits nitric oxide synthesis in cells[22, 23]. Thus, arginine deprivation can't damage mitochondria by increasing nitric oxide biosynthesis in cells. David K. Ann and Hsing-Jien Kung[24] also reported that mitochondria damage is the major reason of cancer cell apoptosis aroused by ADI-PEG20. Our MPTP experiments also proved that ADI expressed in cytosol led to serious mitochondria damage as shown in fig 4c. However, it is still unknown for the apoptosis pathway induced by mitochondrial damage during arginine deprivation.

Then we checked the expression of some protein factors relating with mitochondria apoptosis pathway. As shown in fig 4a and 4b, 2 days of arginine deprivation increased the expression of p53 and p53AIP1 proteins in PC3 and HepG2 cells. The ectopic expression of p53AIP1 protein will induce the down-regulation of mitochondrial $\Delta\psi_m$ (transmembrane potential) and the release of cytochrome c from mitochondrial by interacting and inhibiting Bcl-2 at mitochondrial[25]. Obviously, after two days starvation, the up-regulated p53AIP1 protein activated the p53-dependent apoptosis by interacting with the up-regulated p53 protein[11, 26]. Then cytochrome C was released from mitochondrial. Casp9 and Casp3 were activated as shown in fig 4d and 4e. At the later stage of arginine deprivation (for 4 days), PC3 and HepG2 cells seemed to enter the initiative apoptosis process, because the increasing expression

of Noxa, PUMA, Bax and Bak proteins would further aggravate mitochondria damage[27, 28] as shown in fig 4a and 4b.

We further knocked down the mRNA levels of p53 and p53AIP1 to verify their action during arginine deprivation. As shown in fig 5a, 5b, 5d and supplementary fig S5, the knock-down effectively decreased the apoptosis rates in PC3 and HepG2 cells. p53 knock-down displayed the better effects on apoptosis inhibition than p53AIP1 knock-down. Mitochondria damage was also prevented by p53 knock-down, due to the higher fluorescence intensity of living cells exhibiting in fig 5c. Therefore, p53-dependent apoptosis pathway was the major pathway induced by ADI expressed in cytosol.

Mitochondria damage is not the only way to result in cancer cell death during arginine deprivation in cells. Cell autophagy was reported to be induced by ADI-PEG20[16]. Autophagy, the process of cellular self-eating, is usually caused by starvation or stress, which is capable to degrade long-lived proteins and organelles such as endoplasmic reticulum, mitochondria, peroxisomes, ribosomes and nucleus[29, 30]. We also verified that autophagy was aroused by cytosolic ADI. pEGFP-LC3 and pcDNA4-ADI plasmids were co-transfected into cells. With the expression of ADI, the more proteins were converted from LC3-I to LC3-II as shown in figure 6b. Cytosolic GFP-LC3-I will be conjugated to phosphatidylethanolamine to form GFP-LC3-II during autophagy. GFP-LC3-II will be recruited to autophagosomal membranes with the formation of autophagosomes[31]. As shown in figure 6a, green GFP fluorescent particles presenting around the nucleus were autophagosomes in two cancer cells. Thus, with the expression of ADI, the autophagy aroused by arginine deprivation was indeed taking place in the cells.

Hsing-Jien Kung reported that arginine deprivation *in vitro* will lead to cancer cell chromatin autophagy[32]. He indicated that prolonged arginine deprivation causes mitochondria dysfunction and ROS generation, eventually resulting in nuclear DNA damage and membrane remodeling. Excessive autophagy leads to giant aggregate of autophagosomes/autolysosomes fusion at the later time point of arginine deprivation *in vitro*. Stephen Gregory[33] disclosed that chromatophagy is necessary for the survival of chromosomal instability (CIN) cells. Chromatophagy is activated to remove the defective mitochondria in response to DNA damage. However, we had an additional view about the chromatophagy. We think that arginine deficiency will mobilize cells to utility endogenous arginine storage. Nucleosome, especially histone 3 (H3), contains abundant arginine residues. Therefore, cells will have to obtain arginine from chromatophagy to maintain basic physiology during arginine deprivation. As shown in fig 6f, nucleus budding presented in HepG2 and PC3 cells after the co-transfection of pcDNA4-ADI and pEGFP-LC3 for 96 hours. Chromatin fragment (blue fluorescence) and H3 proteins (red fluorescence) were displayed to co-localize in autophagosomes (GFP green fluoresence). This showed that cytosolic ADI also aroused chromatin autophagy. H3 proteins presenting in autophagosomes implied the utility of histones arginine.

Hence, we have a hypothesis about how cytosolic ADI causes cancer cell death. Cytosolic ADI leads the rapid deprivation of cytosolic arginine, which promote cancer cells to utilize the endogenous arginine. Cancer cells start chromatin autophagy to use the arginine richly existing in nucleosomes. At the early

stage of arginine deprivation, chromatin autophagy is tiny, but DNA damage activate the expression increase of p53 and p53AIP1 proteins. The interaction of p53 and p53AIP1 further aggravates mitochondria damage. At the later stage of arginine deprivation, the accumulation of chromatin autophagy makes DNA damage worse, which arouses the expression increase of Noxa, PUMA, Bax and Bak proteins. Mitochondria damage is irretrievable this time. Cancer cells get into irreversible death, too.

Conclusion

Based on the above discussion, we can see that cancer cells death is primarily induced by rapid arginine deprivation when ADI gene is expressed in cytoplasm. Mitochondria damage is the main death pathway aroused by rapid arginine deprivation. The interaction of ADI and FTL has only a limited effect on mitochondria damage. With the continuous arginine deprivation, the formation of chromatin autophagy aggravates DNA damage. The p53-dependent apoptosis pathway is fully activated, and then cancer cells die.

Abbreviations

ADI: Arginine deiminase; ADI-PEG20: Pegylated Arginine Deiminase by PEG 20,000; FTL: ferritin light-chain domain; H3: Histone 3; ASS: argininosuccinate synthetase; HCC: hepatocellular carcinoma; hTERT: human telomerase reverse transcriptase; cDNA: complementary DNA: qRT-PCR: quantitative reverse transcription-polymerase chain reaction; co-IP: Co-immunoprecipitation; LC3: microtubule-associated protein 1A/1B-light chain 3; LC3-II: LC3-phosphatidylethanolamine conjugate; CIN cells: chromosomal instability cells

Declarations

Ethics approval and consent to participate

Not applicable

Consent for publication

Not applicable.

Availability of data and materials

Not applicable.

Competing interests

The authors declare that they have no competing interests.

Funding

This work was supported by Grants from National Natural Science Foundation of China (Nos. 30800190, 81372441), and State Key Laboratory of Virology of China. The funder played the role in designing the study, in supervising the experiments, and in writing the manuscript.

Author information

Author notes

Qingyuan Feng, Xuzhao Bian and Xuan Liu contributed equally to this work.

Affiliations

Qingyuan Feng[2*,email], Xuzhao Bian[1*,email], Xuan Liu[1*,email], Ying Wang[1,email], Huiting Zhou[1,email], Xiaojing Ma[1,email], Chunju Quan[1,email], Yi Yao[3,email], Zhongliang Zheng[1#,email]

1. State Key Laboratory of Virology, College of Life Sciences, Wuhan University, Wuhan 430072, China.
2. Department of Otorhinolaryngology Head and Neck Surgery, the First Affiliated Hospital of Guangxi Medical University, Nanning, Guangxi 530021, China
3. Department of Oncology, Renmin Hospital of Wuhan University, Wuhan 430060, China

Authors Contributions

XB, QF and XL did most experiments, wrote the manuscript; YW and HZ participated in plasmid construction and cell culture; XM participated in autophagy assay and flow cytometer assay; CQ helped to prepare real-time PCR and Western Blot; YY performed the statistical analyses and revised the manuscript; XB, QF, XL and ZZ conceived and designed the overall study, supervised the experiments, and wrote the paper. All authors read and approved the final manuscript.

Corresponding authors

Correspondence to Zhongliang Zheng

Acknowledgments

The authors thanks Youjun Li and Min Wu for plasmid supply.

References

1. Jiang H, Guo S, Xiao D, Bian X, Wang J, Zheng Z: **Arginine deiminase expressed in vivo displayed higher hepatoma targeting and oncolytic efficiency, which was driven by human telomerase reverse transcriptase promoter**. *Oncotarget* 2017, **8**(23):37694-37704.
2. Yadav L, Puri N, Rastogi V, Satpute P, Sharma V: **Tumour Angiogenesis and Angiogenic Inhibitors: A Review.** *J Clin Diagn Res* 2015, **9**(6):XE01–XE05.
3. Izzo F, Marra P, Beneduce G, Castello G, Vallone P, Rosa VD, Cremona F, Ensor CM, Holtsberg FW, Bomalaski JS *et al*: **Pegylated Arginine Deiminase Treatment of Patients With Metastatic Melanoma: Results From Phase I and II Studies**. *Journal of Clinical Oncology* 2005, **23**(30):7660-7668.
4. Glazer ES, Piccirillo M, Albino V, Giacomo RD, Palaia R, Mastro AA, Beneduce G, Castello G, Rosa VD, Petrillo A *et al*: **Phase II Study of Pegylated Arginine Deiminase for Nonresectable and Metastatic Hepatocellular Carcinoma**. *Journal of Clinical Oncology* 2010, **28**(13):2220-2226.
5. Dillon BJ, Prieto VG, Curley SA, Ensor CM, Holtsberg FW, Bomalaski JS, Clark MA: **Incidence and distribution of argininosuccinate synthetase deficiency in human cancers, A method for identifying cancers sensitive to arginine deprivation**. *Cancer* 2004, **100**(4):826-833.
6. Changou CA, Chen Y-R, Xing L, Yen Y, Chuang FYS, Cheng H, Bold RJ, Ann DK, Kung H-J: **Arginine starvation-associated atypical cellular death involves mitochondrial dysfunction, nuclear DNA leakage, and chromatin autophagy**. *PNAS* 2014, **111**(39):14147-14152.
7. Qiu F, Chen Y-R, Liu X, Chu C-Y, Shen L-J, Xu J, Gaur S, Forman HJ, Zhang H, Zheng S *et al*: **Arginine Starvation Impairs Mitochondrial Respiratory Function in ASS1-Deficient Breast Cancer Cells**. *Sci Signal* 2014, **7**(319):1-10.
8. Szlosarek PW, Luong P, Phillips MM, Baccarini M, Ellis S, Szyszko TA, Sheaff M, Avril N: **Metabolic Response to Pegylated Arginine Deiminase in Mesothelioma With Promoter Methylation of Argininosuccinate Synthetase**. *J Clin Oncol* 2013, **31**(7):111-113.
9. Abou-Alfa GK, Qin S, Ryoo BY, Lu SN, Yen CJ, Feng YH, Lim HY, Izzo F, Colombo M, Sarker D *et al*: **Phase III randomized study of second line ADI-PEG 20 plus best supportive care versus placebo plus best supportive care in patients with advanced hepatocellular carcinoma.** *Ann Oncol* 2018, **29**(6):1402-1408.
10. Das K, Butler GH, Kwiatkowski V, Arthur D. Clark J, Yadav P, Arnold E: **Crystal Structures of Arginine Deiminase with Covalent Reaction Intermediates: Implications for Catalytic Mechanism**. *Struture* 2004, **12**:657-667.

11. Oda K, Arakawa H, Tanaka T, Matsuda K, Tanikawa C, Mori T, Nishimori H, Tamai K, Tokino T, Nakamura Y *et al*: **p53AIP1, a Potential Mediator of p53-Dependent Apoptosis, and Its Regulation by Ser-46-Phosphorylated p53**. *Cell* 2000, **102**:849-862.
12. Rabinowitz JD, White E: **Autophagy and Metabolism**. *Science* 2010, **330**(6009):1344-1348.
13. Tanida I, Waguri S: **Measurement of Autophagy in Cells and Tissues**. *Methods Mol Biol* 2010, **648**:193-214.
14. Simone BA, Champ CE, Rosenberg AL, Berger A, Monti DA, Dicker AP, Simone NL: **Selectively starving cancer cells through dietary manipulation: methods and clinical implications**. *Future Oncol* 2013, **9**(7):959-976.
15. Ohshima K, Nojima S, Tahara S, Kurashige M, Hori Y, Hagiwara K, Okuzaki D, Oki S, Wada N, Ikeda J-i *et al*: **Argininosuccinate Synthase 1-Deficiency Enhances the Cell Sensitivity to Arginine through Decreased DEPTOR Expression in Endometrial Cancer**. *Scientific Reports* 2017, **30**(7):45504-45518.
16. Randie HK, Jodi MC, Tawnya LB, Gregory PM, Julie S, Kung HJ et al: **Arginine Deiminase as a Novel Therapy for Prostate Cancer Induces Autophagy and Caspase-Independent Apoptosis**. *Cancer Research* 2009, **69**(2):700-708.
17. Arosio P, Elia L, Poli M: **Ferritin, cellular iron storage and regulation**. *IUBMB Life* 2017, **69**(6):414-422.
18. Richardson DR, Lane DJR, Becker EM, Huang ML-H, Whitnall M, Rahmanto YS, Sheftel AD, Ponkac P: **Mitochondrial iron trafficking and the integration of iron metabolism between the mitochondrion and cytosol**. *PNAS* 2010, **107**(24):10775-10782.
19. Lu X, Galkin A, Herzberg O, Dunaway-Mariano D: **Arginine Deiminase Uses an Active-Site Cysteine in Nucleophilic Catalysis of l-Arginine Hydrolysis**. *Journal of the American Chemical Society* 2004, **126**(17):5374-5375.
20. Szlosarek PW: **Arginine deprivation and autophagic cell death in cancer.** *PNAS* 2014, **111**(39):14015-14016.
21. Savaraj N, You M, Wu C, Wangpaichitr M, Kuo MT, Feun LG: **Arginine Deprivation, Autophagy, Apoptosis (AAA) for the Treatment of Melanoma**. *Current Molecular Medicine* 2010, **10**(4):405-412.
22. Sezgin N, Torun T, Yalcin F: **Biochemical characterization of the arginine degrading enzymes arginase and arginine deiminase and their effect on nitric oxide production.** *Med Sci Monit* 2002, **8**(10):LE44-40.
23. Zou S, Wang X, Liu P, Ke C, Xu S: **Arginine metabolism and deprivation in cancer therapy**. *Biomedicine & Pharmacotherapy* 2019, **118**:1-11.
24. Cheng C-T, Qi Y, Wang Y-C, Chi KK, Chung Y, Ouyang C, Chen Y-R, Oh ME, Sheng X, Tang Y *et al*: **Arginine starvation kills tumor cells through aspartate exhaustion and mitochondrial dysfunction**. *Communication Biology* 2018, **1**(178):1-19.
25. Matsuda K, Yoshida K, Taya Y, Nakamura K, Nakamura Y, Arakawa H: **p53AIP1 Regulates the Mitochondrial Apoptotic Pathway**. *Cancer Research* 2002, **62**(10):2883-2889.

26. O'Prey J, Crighton D, Martin AG, Vousden KH, O.Fearnhead H, Ryan KM: **p53-mediated induction of Noxa and p53AIP1 requires NFκB**. *Cell Cycle* 2010, **9**(5):947-952.
27. Vaseva AV, Moll UM: **The mitochondrial p53 pathway**. *Biochimica et Biophysica Acta* 2009, **1787**:414-420.
28. Brenner C, Galluzzi L, Kepp O, Kroemer G: **Decoding cell death signals in liver inflammation**. *Journal of Hepatology* 2013, **59**(3):583-594.
29. Stolz A, Ernst A, Dikic I: **Cargo recognition and trafficking in selective autophagy**. *Nature Cell Biology* 2014, **16**:495-501.
30. Kaur J, Debnath J: **Autophagy at the crossroads of catabolism and anabolism** *Moledular Cell Biology* 2015, **16**:461-472.
31. Zhang Z, Singh R, Aschner M: **Methods for the Detection of Autophagy in Mammalian Cells**. *Curr Protoc Toxicol* 2016, **69**(1):20.12.21-20.12.26.
32. Kung H-J, Changou CA, Li C-F, Ann DK: **Chromatophagy: Autophagy goes nuclear and captures broken chromatin during arginine-starvation**. *Autophagy* 2015, **11**(2):419-421.
33. Liu D, Shaukat Z, Xu T, Denton D, Robert Saint3, Gregory S: **Autophagy regulates the survival of cells with chromosomal instability**. *Oncotarget* 2016, **7**(39):63913-63923.

Additional Information

Supplementary information

Additional file 1: Original Western Blot results and some primers for qPCR. Fig S1 is associated with fig 1c. Fig S2 is associated with fig 2b. Fig S3 is associated with fig 3d. Fig S4 is associated with fig 4b. Fig S5 is associated with fig 5d. Fig S6A is associated with fig 6b. Fig S6B is associated with fig 6d. Tab S1 displays some primers for qPCR experiments

Figures

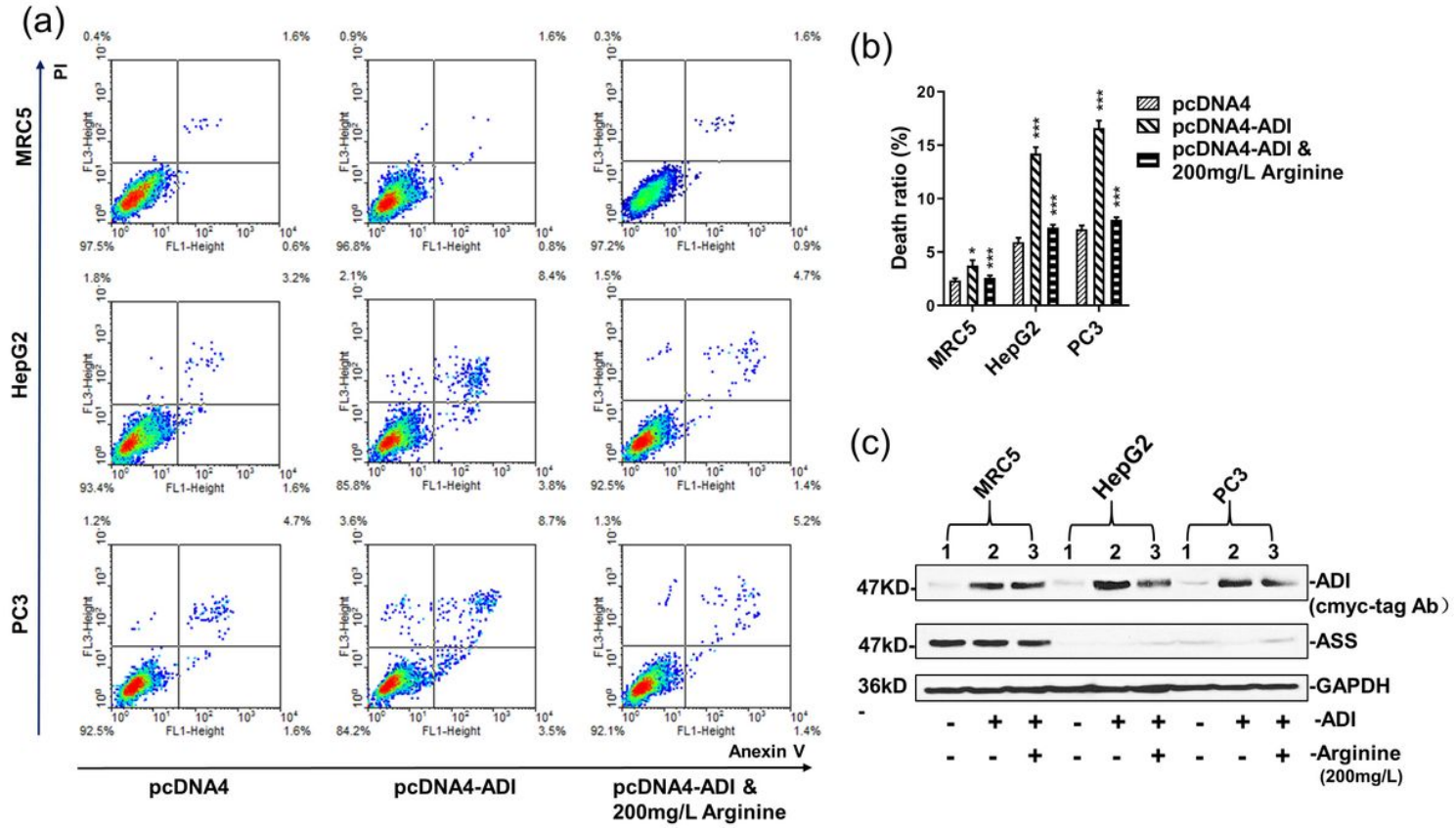

Figure 1

Apoptosis efficiency induced by ADI expressed in MRC5, HepG2 and PC3 cells. Cells were separately transfected by pcDNA4, pcDNA4-ADI plasmids. Cell apoptosis rates were detected by flow cytometry after the static cell culture for 48h. a: Representative images of FACS analysis of annexin V and PI staining of MRC5, HepG2 and PC3 cells. b: Death ratio summary of FACS analysis from fig 1a. c: Immunoblots of ADI and ASS expression in MRC5, HepG2 and PC3 cells. C-myc-tag antibody was used to detect c-myc-tag-fused ADI. The blot of GAPDH was from the same gel as the blot of ADI. The original blot results were from supplementary fig S1.

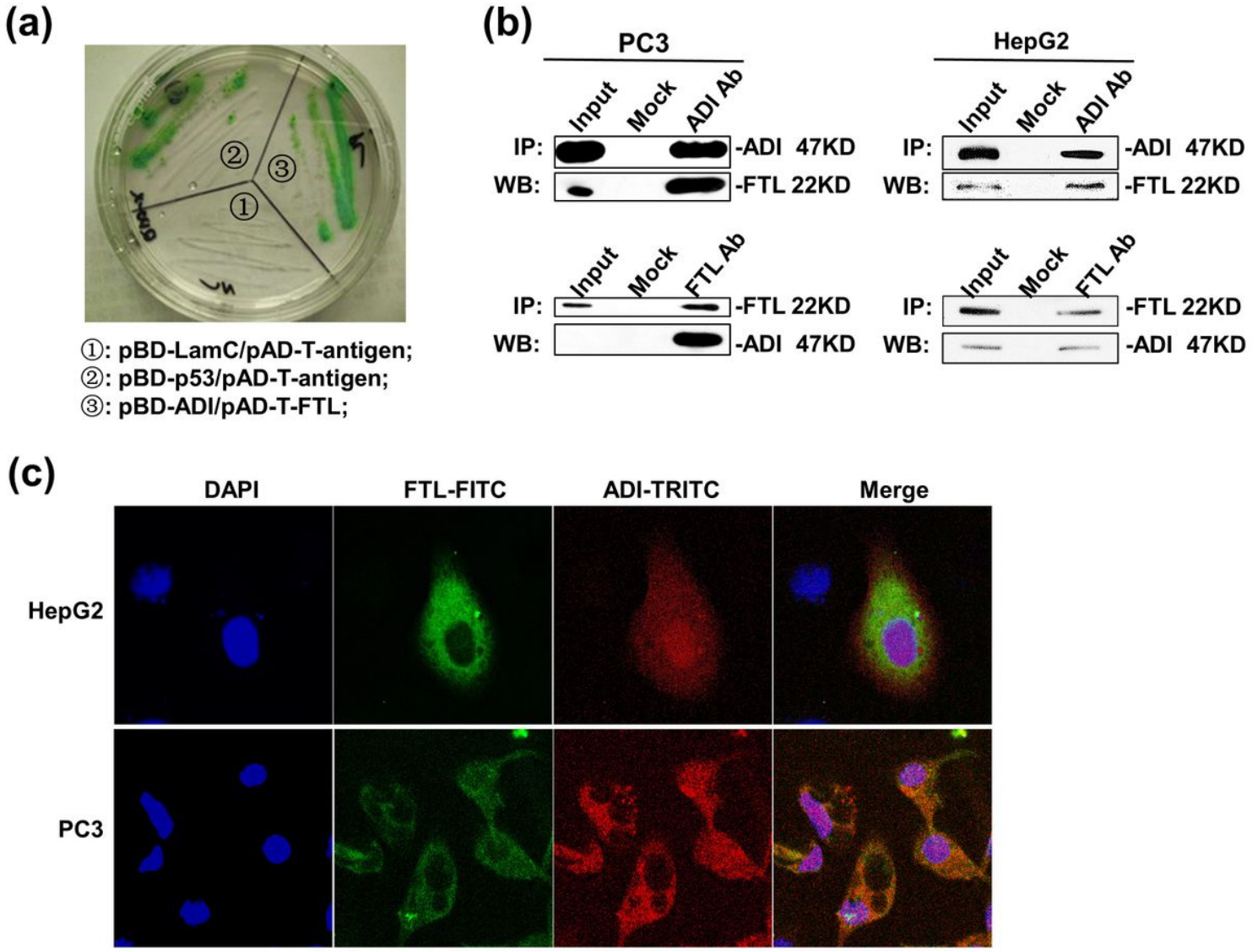

Figure 2

The interaction of ADI and FTL in cells. a: Yeast were co-transformed with pBD-ADI and pAD-T-FTL plasmid, and grew on an SD agar plate with high-stringency nutrient selection (SD/-Leu/-Trp/-His/-Ade). pBD-LamC/pAD-T-antigen plasmids were used as negative control. pBD-p53/pAD-T-antigen plasmids were used as positive control. b: Co-IP of ADI or FTL was applied by antibodies specific for ADI or FTL. Images represent the immuneprecipitates separated by SDS-PAGE and incubated with the indicated antibodies. The blots of each line were from the same gel. The original blot results were from supplementary fig S2. c: Immunofluorescence staining of HepG2 and PC3 cells with antibody against ADI (red) and antibody against FTL (green). Cells were transfected with pcDNA4-ADI plasmid. The fluorescence was detected on an inverted fluorescence microscope.

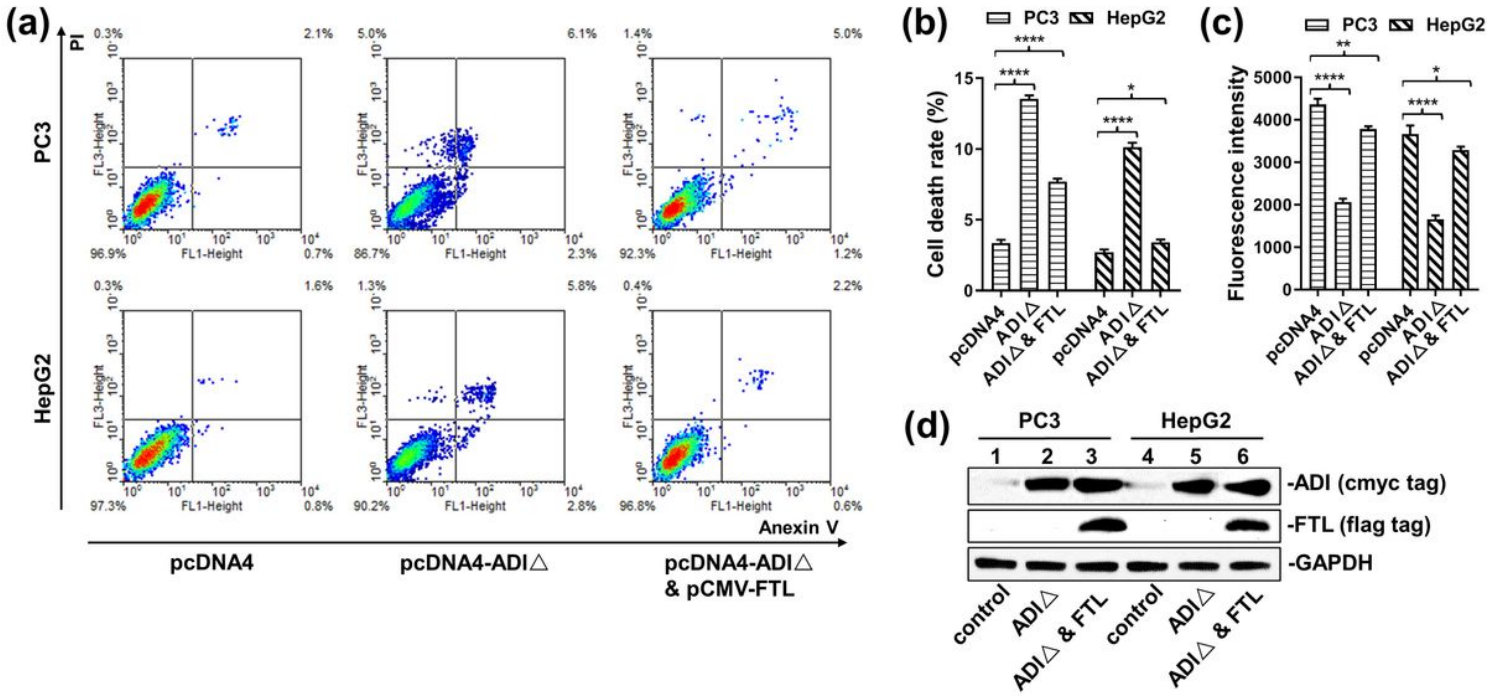

Figure 3

Apoptosis efficiency induced by ADI△(C398A) expressed in MRC5, HepG2 and PC3 cells. Cells were separately transfected by pcDNA4, pcDNA4-ADI△ and pCMV-FTL plasmids. Cell apoptosis rates were detected by flow cytometry after the static cell culture for 72h. a: Representative images of FACS analysis of annexin V and PI staining of MRC5, HepG2 and PC3 cells. b: Death ratio summary of FACS analysis from fig 3a. c: Fluorescence assay for mitochondrial permeability transition pore (MPTP) from fig 3a. d: Immunoblots of ADI△ and ASS expression in MRC5, HepG2 and PC3 cells. C-myc-tag antibody was used to detect c-myc-tag-fused ADI△. FLAG tag was used to detect overexpressed FTL. The blot of GAPDH was from the same gel as the blot of FTL. The original blot results were from supplementary fig S3

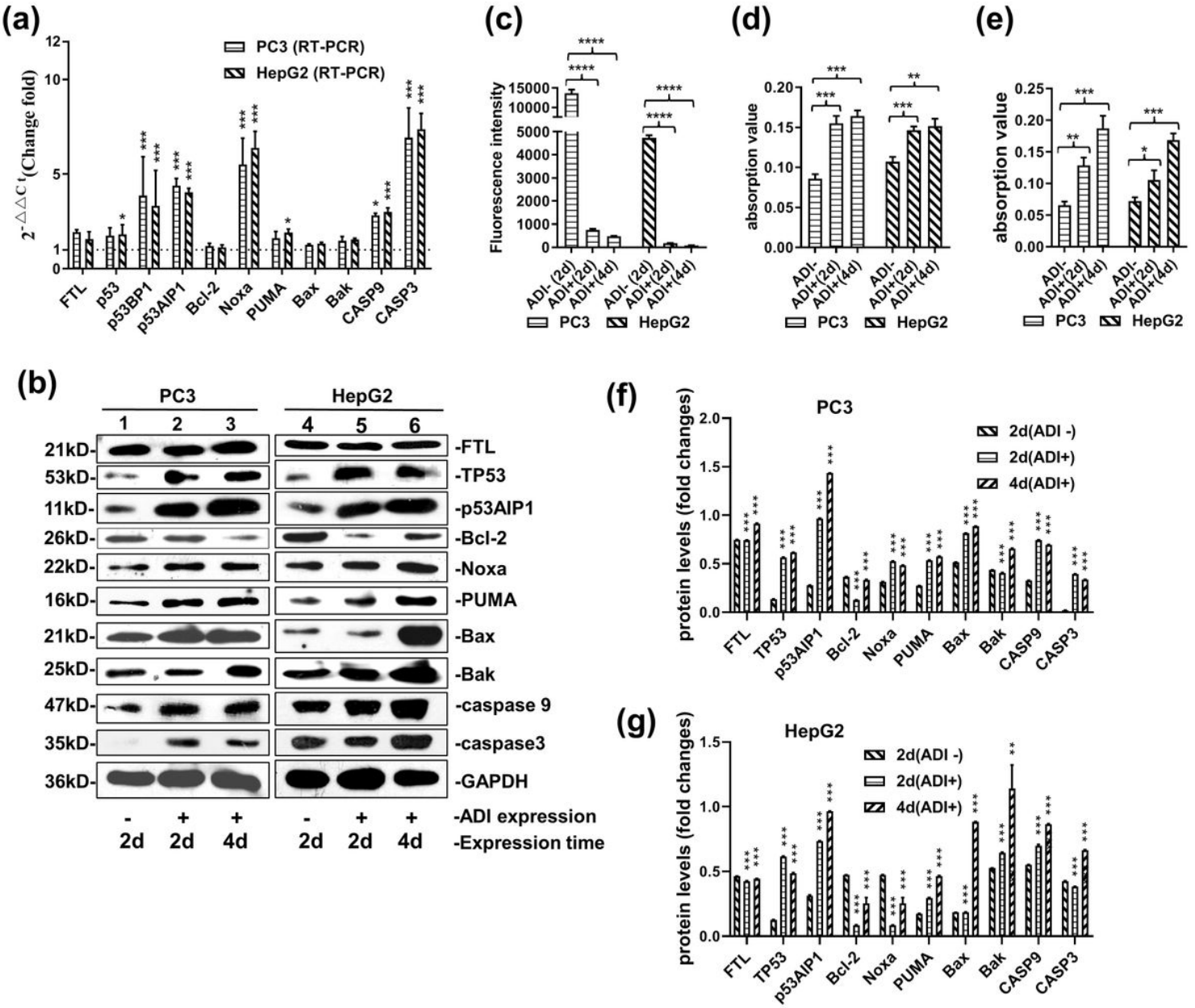

Figure 4

Molecular mechanism of cell apoptosis induced by arginine deprivation. a: mRNA level detection of some factors related with mitochondria apoptosis pathway by Quantitative RT-PCR in PC3 and HepG2 cells. b: Immunoblot of the factors related with apoptosis pathway in PC3 and HepG2 cells. The original blot results were from supplementary fig S4. c: Fluorescence assay for mitochondrial permeability transition pore (MPTP). d: Activity assay of Caspase 3 through caspase 3 assay kit (Colorimetric) (abcam. ab39401). e: Activity assay of Caspase 9 through caspase 9 assay kit (Colorimetric) (abcam. Ab65608). f/g: the relative quantification for protein expressions in PC3 and HepG2 cell lines. Grey scales of protein bands from fig 4b were detected by ImageJ 1.52. P values were calculated by comparing pcDNA4-ADI plasmids-treated cells with pcDNA4 plasmid-treated cells in the respective cell lines. **P < 0.01; ***P < 0.001.

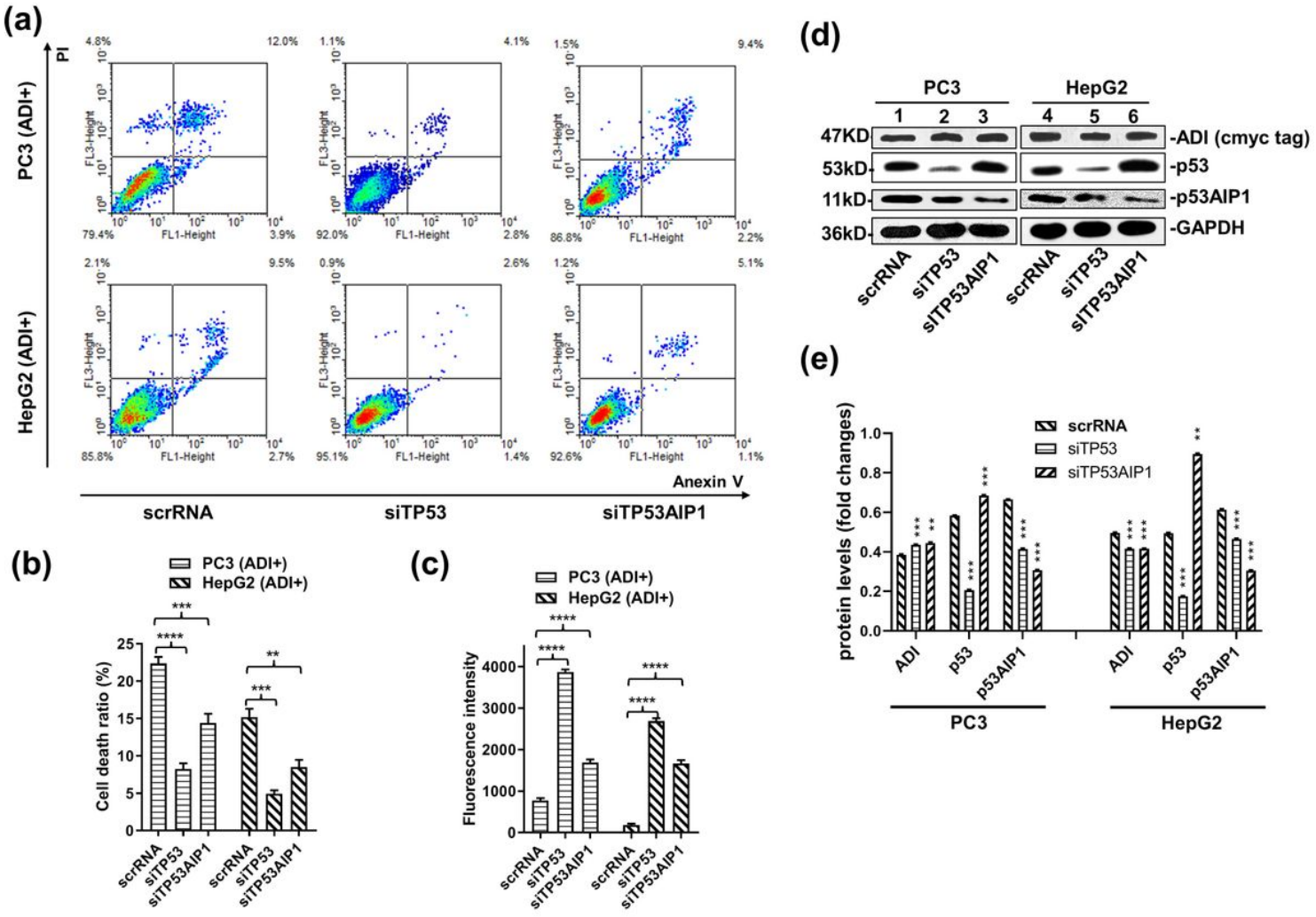

Figure 5

The effect of knock-down of p53 and p53AIP1 genes on apoptosis efficiency induced by ADI. Cells were separately co-transfected by pcDNA4-ADI plasmids with siTP53 or siTP53AIP1. Cell apoptosis rates were detected by flow cytometry after the static cell culture for 48h. a: Representative images of FACS analysis of annexin V and PI staining of HepG2 and PC3 cells. b: Death ratio summary of FACS analysis from fig 5a. c: Fluorescence assay for mitochondrial permeability transition pore (MPTP) from fig 3a. d: Immunoblots of ADI, p53 and p53AIP1 protein expression in HepG2 and PC3 cells. C-myc-tag antibody was used to detect c-myc-tag-fused ADI. The original blot results were from supplementary fig S5. e: the relative quantification for protein expressions in PC3 and HepG2 cell lines. Grey scales of protein bands from fig 5d were detected by ImageJ 1.52. P values were calculated by comparing siRNA-treated cells with scrRNA-treated cells in the respective cell lines. **P < 0.01; ***P < 0.001.

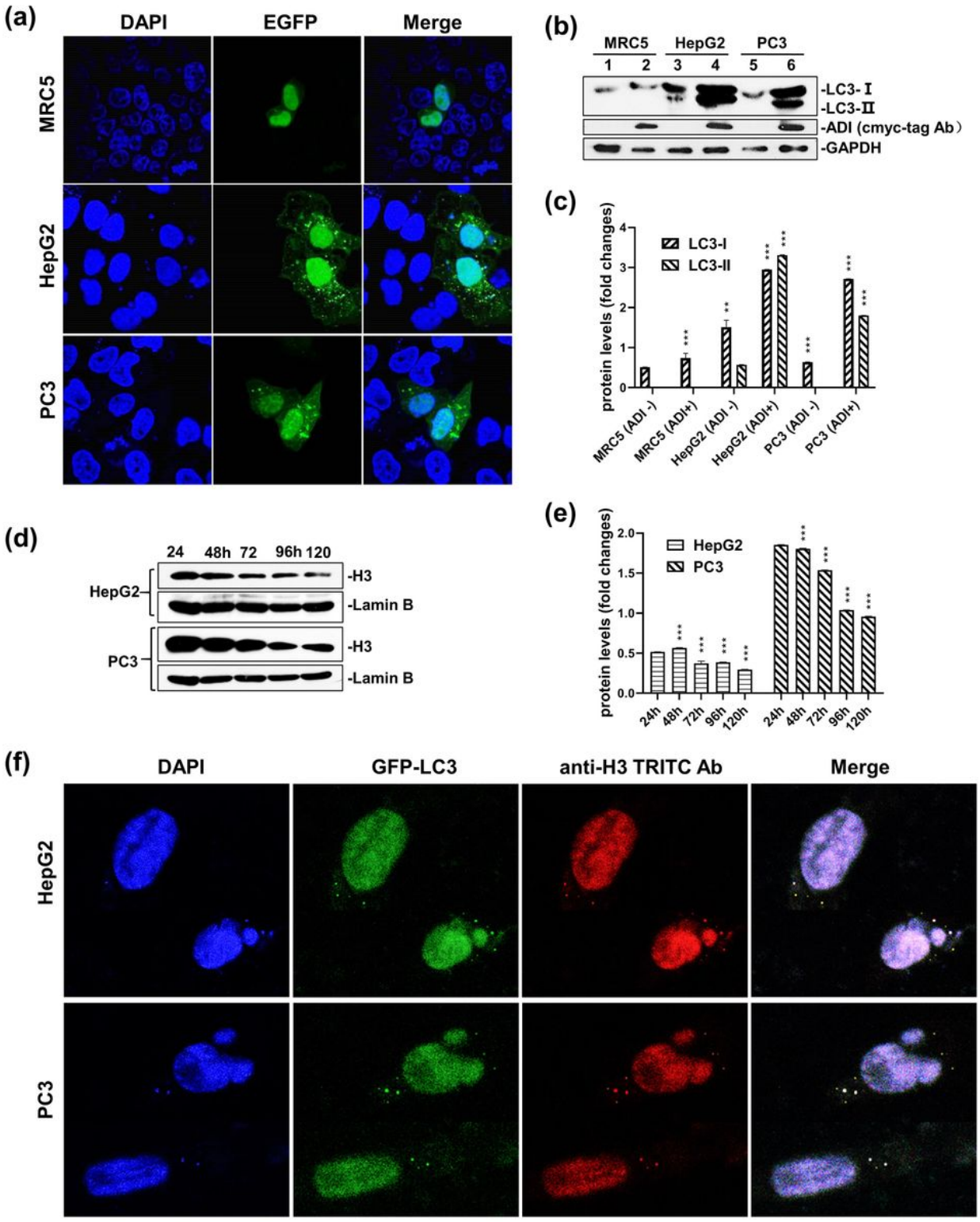

Figure 6

Chromatin autophagy assay at the later time point of arginine deprivation. a: GFP-LC3 reporter fluorescence assay for autophagy in MRC5, HepG2 and PC3 cells. Cells were co-transfected with pcDNA4-ADI plasmid and pEGFP-LC3 plasmid. The fluorescence of EGFP protein was detected by OLIMPUS inverted fluorescence microscope SteREO Discovery V12. b: Immunoblot of LC3-I and LC3-II in MRC5, HepG2 and PC3 cells. Cells were treated as the description of fig 6a. LC3 antibody was used to detect

LC3-I and LC3-II proteins. C-myc-tag antibody was used to detect c-myc-tag-fused ADI. The original blot results were from supplementary fig S6A. c: the relative quantification for protein expressions in MRC5, PC3 and HepG2 cell lines. Grey scales of protein bands from fig 6b were detected by ImageJ 1.52. P values were calculated by comparing pcDNA4-ADI plasmids-treated cells with pcDNA4 plasmid-treated cells in the respective cell lines. **P < 0.01; ***P < 0.001. d: Immunoblots of H3 protein expression in HepG2 and PC3 cells. Cells were transfected with pcDNA4-ADI plasmid. Histone H3 antibody (Cat. # 17168-1-AP) were used to detect H3 protein. The original blot results were from supplementary fig S6B. e: the relative quantification for protein expressions in MRC5, PC3 and HepG2 cell lines. Grey scales of protein bands from fig 6d were detected by ImageJ 1.52. P values were calculated by comparing other cells with 24h-treated cells in the respective cell lines. **P < 0.01; ***P < 0.001. f: Immunofluorescence assay for chromatin autophagy. Cells were cultured in DMEM medium with 2% FBS. Histone H3 antibody (Cat. # 17168-1-AP) were used to detect H3 protein in cells. TRITC conjugated goat anti-rabbit antibody (Cat. # A16101) was used to detect H3 antibody and display the immunofluorescence.

Supplementary Files

This is a list of supplementary files associated with this preprint. Click to download.

- Supplementaryinformation.pdf